ELSEVIER

Journal of Nuclear Materials 313–316 (2003) 573–578

journal of nuclear materials

www.elsevier.com/locate/jnucmat

Core fueling and edge particle flux analysis in ohmically and auxiliary heated NSTX plasmas

V.A. Soukhanovskii [a,*], R. Maingi [b], R. Raman [c], H.W. Kugel [a], B.P. LeBlanc [a], A.L. Roquemore [a], C.H. Skinner [a], NSTX Research Team

[a] Princeton Plasma Physics Laboratory, MS-15, P.O. Box 451, Princeton, NJ 08543, USA
[b] Oak Ridge National Laboratory, Oak Ridge, TN 37831, USA
[c] University of Washington, Seattle, WA 98195, USA

Abstract

The Boundary Physics program of the National Spherical Torus Experiment (NSTX) is focusing on optimization of the edge power and particle flows in $\beta_t \geqslant 25\%$ L- and H-mode plasmas of $t \leqslant 0.8$ s duration heated by up to 6 MW of high harmonic fast wave and up to 5 MW of neutral beam injection (NBI). Particle balance and core fueling efficiencies of low and high field side gas fueling in L-mode ohmic and NBI-heated plasmas have been compared using an analytical zero-dimensional particle balance model and measured ion and neutral fluxes. Gas fueling efficiencies are in the range of 0.05–0.20 and do not depend on discharge magnetic configuration, density or poloidal location of the injector. The particle balance modeling indicates that the addition of a pseudo-constant high field side (HFS) fueling source results in a reversal of the wall loading rate and higher wall inventories. Initial particle source estimates obtained from neutral pressure and spectroscopic measurements indicate that the recycling flux in the divertor exceeds the main chamber ion and neutral fluxes by over an order of magnitude. Present analysis provides the basis for detailed fluid modeling of edge heat and particle flows using transport models which include both diffusion and convection.

Keywords: Spherical torus; Fueling; Particle balance; NSTX

1. Introduction

The focus of the National Spherical Torus Experiment (NSTX) Boundary Physics program is the optimization of the edge power and particle flows in $\beta_t \geqslant 25\%$ long pulse L- and H-mode plasmas heated by up to 6 MW of high harmonic fast wave (HHFW) power and up to 5 MW of neutral beam injection (NBI). It has been initially thought that conventional tokamak power and particle handling techniques would be challenged by the spherical tori (ST) features, such as the compactness of the divertor and the scrape-off layer (SOL) width, resulting from the short connection length and high mirror ratio (for example, [1]). NSTX has successfully achieved NBI heated and HHFW heated H-mode plasmas of several τ_E duration and stored energy up to $E \leqslant 200$ kJ and plasmas with $\beta_t \leqslant 30\%$ thus demonstrating that the conventional techniques are adequate for $t \leqslant 0.8$ s duration high performing ST target plasma. The purpose of this paper is to provide an initial analysis of global particle balance in NSTX and an assessment of the efficiency of the core fueling and divertor performance. This global approach helps identify the directions for further detailed analysis of particle confinement, core density limiting mechanisms, and scrape-off layer transport, involving multi-fluid numerical modeling of edge plasmas [2].

* Corresponding author. Fax: +1-609 243 2665.
E-mail address: vlad@pppl.gov (V.A. Soukhanovskii).

0022-3115/03/$ - see front matter © 2003 Elsevier Science B.V. All rights reserved.
PII: S0022-3115(02)01413-7

2. Experiment and diagnostics

External fueling of NSTX plasmas is achieved by neutral gas injectors and neutral beam injectors. Top and outer midplane fast piezoelectric valves are referred to as the low field side (LFS) injectors. The valves provide a well-controlled continuous gas flow at a rate $\Gamma_{gas} \leqslant 170$ Torr l/s per injector. The high field side (HFS) gas injector was recently installed on NSTX following the successful MAST demonstration of improved H-mode access with inner wall gas fueling [3]. The gas injector provides a pseudo-constant flow at a rate $\Gamma_{gas} \leqslant 50$ Torr l/s. Three $E \leqslant 90$ keV deuterium beams injected co-directionally with plasma current at three radii of $r_1 = 48.7$, $r_2 = 59.2$, $r_3 = 64.9$ cm yield a fueling rate of $\Gamma_{NBI} \simeq 1.3$ Torr l/s per 1 MW of NBI power.

Quantitative particle balance analysis utilizes the measurements of several diagnostics. These are fast neutral pressure gauges, including two calibrated ionization gauges in the midplane, and two Penning gauges in upper and lower divertors. Plasma profiles are measured by a multi-point Thomson scattering system. Various spectroscopic diagnostics include filtered detectors of impurity, visible bremsstrahlung, and the deuterium Balmer line emissions, and visible and VUV spectrometers. Especially useful for neutral recycling measurements are the photometrically and spatially calibrated 2048-pixel optically filtered CCD arrays, viewing the lower divertor neutralizer plates and the center stack tiles.

A database of about 70 inner wall limited (IWL), lower single null and double null (DN) diverted discharges has been used in the present analysis. The discharges included 0.8–1.0 MA ohmically and NBI heated fiducial L-mode deuterium plasmas, and the L-mode ohmic discharges obtained in a density scan experiment. Fueling efficiencies have been determined in the current ramp-up and flat-top phases of the discharge since many plasmas experience MHD modes or reconnection events altering plasma parameters after reaching I_p flattop (at $t \leqslant 0.25$ s).

3. Fueling efficiency analysis

3.1. Particle balance

A global particle balance equation (PBE) (for example, [4]) is applied to each discharge to analyze core plasma contribution of various particle sources and sinks:

$$\frac{dN_i}{dt} = \Gamma_{gas} + \Gamma_{NBI} + \Gamma_{NBI\text{-}cold} - \Gamma_{NBI\text{-}cryo} - \Gamma_{wall} - \Gamma_{pump} - \frac{dN_n}{dt}. \quad (1)$$

The change in total deuteron inventory dN_i/dt is derived from the measured Z_{eff} and the volume-averaged density $N_e \simeq \bar{n}_e V_p \Gamma_{gas}$ is the total gas injector rate. Γ_{NBI} is the NBI fueling rate, $\Gamma_{NBI\text{-}cold} \simeq 0.25 \times \Gamma_{NBI}$ is the NBI line neutral gas fueling rate, and $\Gamma_{NBI\text{-}cryo}$ is the NBI line cryopump rate. Inclusion of the latter term is important: noticeable effect on plasma performance is observed when the NBI duct is open to NSTX vacuum vessel. It is estimated from the cryopump pumping speed of 5×10^4 L/s and neutral pressure measurements. The last two terms in the RHS PBE are the neutral gas build-up rate dN_n/dt and the turbomolecular pump rate Γ_{pump}. The wall loading rate Γ_{wall} is derived from the balance equation. Integrating the equation yields the cumulative particle inventories. Fueling efficiency is defined as $\eta = N_p/N_{ext}$, where N_p is the total number of particles enclosed by the last closed flux surface, and N_{ext} is the total number of particles introduced externally into the vacuum vessel. Fueling efficiency η characterizes individual source contribution to the global particle inventory, as thermal and fast particle transport and confinement properties are different. Instantaneous fueling efficiency may be defined as $\eta_\tau = (dN_i/dt)\Gamma_{gas}^{-1}$. It is determined by the transitory particle balance and is usually lower than η. Shown in Fig. 1 are the PBE results for a LFS (top injector) fueled DN discharge with the following parameters: $I_p = 1$ MA $P_{NBI} = 1.6$ MW, line average density $\bar{n}_e \simeq 2.55 \times 10^{13}$ cm^{-3}. The wall loading rate is positive through the gas pulse duration indicating strong pumping by the walls. After the gas is shut-off, the balance is dominated by the dN_i/dt term, which slowly falls to 10–20 Torr l/s, but still being larger than the total NBI fueling rate of $\Gamma_{NBI} + \Gamma_{NBI\text{-}cold} \leqslant 2$ Torr l/s. The wall loading rate becomes negative indicating that the wall starts degassing. This behavior is characteristic for most L-mode discharges fueled in the initial phase of the discharge from the LFS injectors. Improved plasma control and a higher central plasma density limit due to fueling have been achieved with LFS + HFS fueling. More importantly, the introduction of LFS + HFS fueling allowed for greater reproducibility and control of the L–H transition and edge localized modes in the H-mode plasmas. Shown in Fig. 2 are the PBE quantities derived for an otherwise similar discharge ($I_p = 1$ MA, $P_{NBI} = 1.6$ MW, line average density $\bar{n}_e \simeq 3.60 \times 10^{13}$ cm^{-3}) with additional fueling from HFS injector. The HFS injection starts at $t = -0.26$ s and produces a fueling rate burst at 0.09 s when the gas pulse reaches the plasma. Thereafter, a pseudo-constant rate of about 20 Torr l/s is maintained from HFS injector through a discharge. This rate is sufficient to change the particle balance so that Γ_{wall} becomes positive, indicating that the wall is pumping. The physical interpretation of this result demonstrates the usefulness and limitations of the modeling with a one reservoir PBE. Recycling of neutrals from the wall is

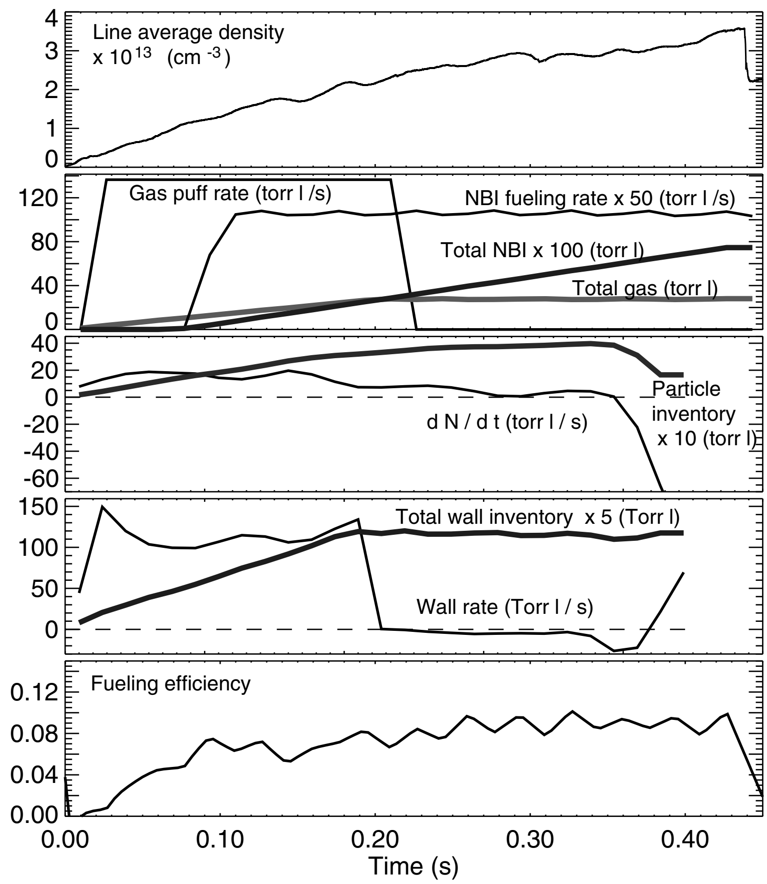

Fig. 1. Particle balance modeling of a LFS fueled discharge.

independent or weakly dependent on external fueling, thus 'pumping' or 'degassing' are interpreted as a net balance of all time-dependent source and sink rates of the particles confined with a finite time τ. More sophisticated multi-reservoir equations include the effects of particle residence time in the SOL, divertor, or the wall surface [2]. For the present fueling analysis, however, the model adequately describes the relative importance of particle sources and sinks in NSTX.

3.2. Gas puff fueling efficiency

In most L-mode discharges that reach $\bar{n}_e \leqslant 5.5 \times 10^{13}$ cm^{-3} and are fueled with $\Gamma_{\rm gas} \leqslant 170$ Torr l/s the deuteron inventory change is $dN_i/dt \leqslant 20$ Torr l/s through the duration of the gas pulse, weakly falling to zero thereafter. Densities as high as $\bar{n}_e \simeq 1.2 \times n_{\rm G}$, the Greenwald density, have been produced by gas puffing from LFS, with $dN_i/dt \leqslant 30$ Torr l/s and limited by an onset of large MHD events or a density-limiting mechanism. Increasing gas injection rate and duration in fueling schemes with LFS only and a combination of LFS and HFS do not tend to change the density (Fig. 3). A combination of LFS and HFS fueling with lower average rates produce higher density plasmas. The average fueling efficiency of gas injectors in NSTX is in the range 0.05–0.20. No significant differences between LFS+HFS and LFS fueling have been found in ohmic and NBI heated L-mode discharges. The fueling efficiency does not seem to have any dependence on gas injector fueling rate. It is also independent of line density for IWL discharges, as shown in Fig. 4. Diverted discharges, however, tend to achieve higher density with higher fueling efficiency. Fueling efficiency for IWL discharges appears to be higher for LFS + HFS fueling scheme. This is closely related to SOL properties and will be further addressed when the measurements of SOL temperature, density and the deuterium ionization profile become available. Finally, we note that the fueling efficiency η has been defined as an average quantity and the present results are valid within the limitations of this definition.

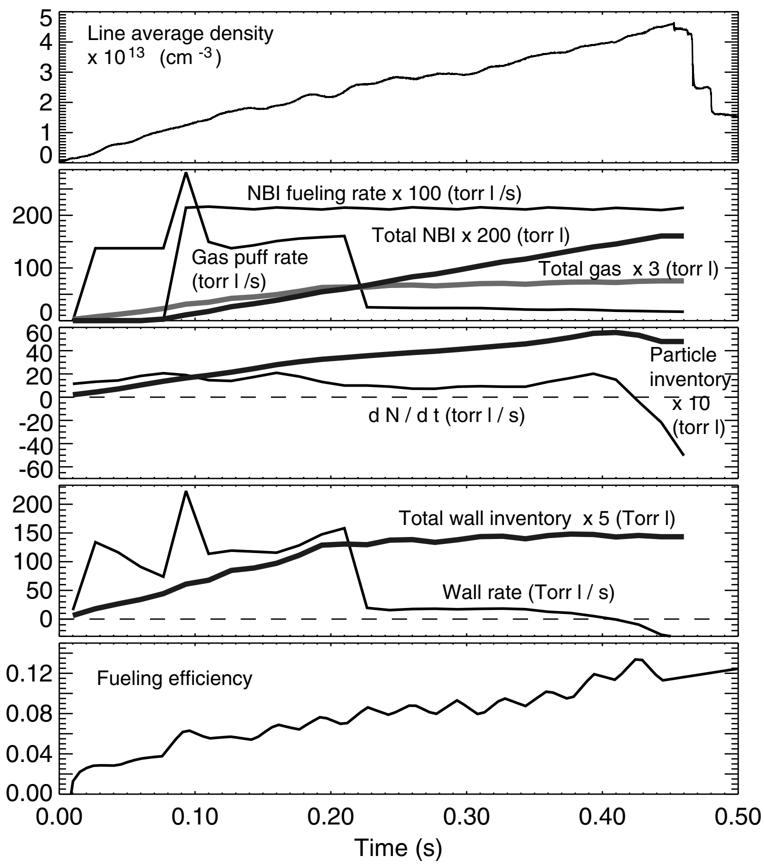

Fig. 2. Particle balance modeling of a LFS + HFS fueled discharge.

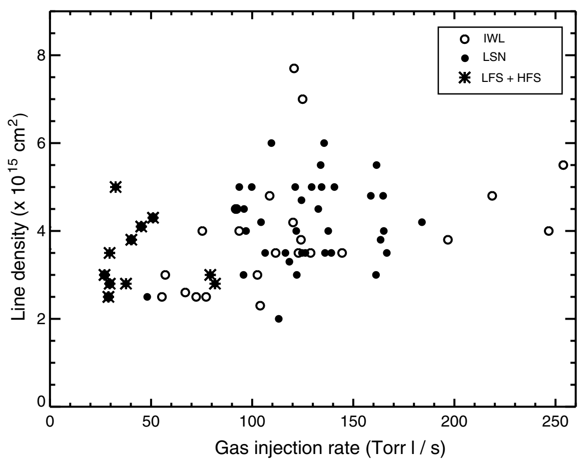

Fig. 3. Line density dependence on gas injection rate.

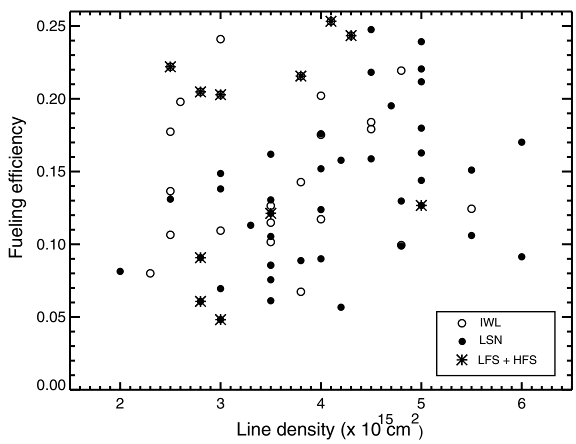

Fig. 4. Gas injection fueling efficiency dependence on line density.

3.3. NBI fueling efficiency

Because of relatively low fueling rate of the NBI it is not possible to determine its fueling efficiency by global particle balance. The ionization profile of NBI is localized well within the core at $r/a \leqslant 0.5$, where a is the minor radius. The estimated beam shine-through for NSTX plasmas is less than 10%.

3.4. Impurity fueling

Main impurities are boron, carbon, and oxygen. Their typical core concentrations after boronization are 0.25–0.5%, 1–1.5%, and 0.1–0.3%, respectively [5]. The effective charge Z_{eff} is between 1.2 and 2.5 in ohmically heated discharges and between 2 and 3.5 in NBI and HHFW heated plasmas. Impurities, therefore, contribute less than 10% to the electron density in NSTX.

4. Comments on edge particle fluxes

At present, NSTX utilizes conventional wall-conditioning techniques for impurity and density control, including boronization and helium glow discharge cleaning [6]. The wall inventory of a 1 MA $t \leqslant 0.5$ s duration NSTX discharge is $\simeq 25$ Torr l. When the wall begins pumping it reduces the total inventory only by about $\leqslant 3$ Torr l. The development of higher performance plasmas will put emphasis on power and particle exhaust capabilities, in particular the divertor performance. NSTX divertor has an open geometry. Whereas the advantages and disadvantages of the geometry over the narrow throat divertors are debatable, it provides only two channels of particle flows: direct particle flow to the divertor plate and direct internal leakage into the main chamber. Detailed divertor characterization will commence at NSTX with commissioning of divertor probes, a bolometer array and Penning gauges. The present assessment of divertor performance is limited to impurity and ion flux estimates obtained from spectroscopic observations. Internal particle source in NSTX is dominated by neutral recycling from the wall. The recycling occurs on carbon fiber composite-tiled surface of the center column with an area $A \leqslant 3.2$ m^2 and the divertor and passive plates with an area $A \leqslant 7$ m^2 (the actual plasma-wetted surface areas are smaller). This section describes observations and preliminary estimates of edge particle fluxes.

4.1. Neutral and ion fluxes

Neutral fluxes are estimated from the pressure measurements assuming poloidal and toroidal symmetry. Ion fluxes are estimated from the measured D_α brightness using the calculated factor of 40 ionization events per D_α photon for NSTX edge parameters $T_e \simeq 20$–40 eV, $n_e \leqslant 5 \times 10^{12}$ cm^{-3}, and the appropriate surface areas. Balmer-α brightness is measured by two 2048-pixel filtered calibrated CCD arrays across the lower divertor and in the midplane across the center stack. It is of interest to compare the magnitude of the ion and neutral fluxes at the midplane and in the divertor region. Shown in Fig. 5 are the average particle fluxes for the HFS + LFS fueled DN discharge analyzed for particle balance in Section 3. The HFS gas injection is seen at 0.08 s and its flux is in agreement with the neutral gas injection rate shown in Fig. 2. Based on a limited database of discharges it is concluded that the ion and neutral flux at the midplane are approximately equal being on the order of 5×10^{21} s^{-1}. The divertor ionization flux is $\leqslant 10^{23}$ s^{-1} assuming that the D_α intensity is directly related to the recycling flux in an attached divertor. Thus, the order of magnitude estimate indicates that the ion flux in the divertor greatly exceeds the ion flux in the midplane. This may indicate that the radial transport near the separatrix and in the SOL is fairly low and the particle flow along the field lines to the divertor is greater than the cross-field flow. The opposite situation has been found recently in the edge of several tokamaks and termed 'main chamber recycling' [7–9]. It has been suggested that strong SOL microturbulence results in a highly non-diffusive particle transport and plasma 'blob' propagation radially outward [9]. Detailed modeling of edge particle and heat fluxes in NSTX using purely diffusive and diffusive–convective transport models shall help with the interpretation of the present measurements.

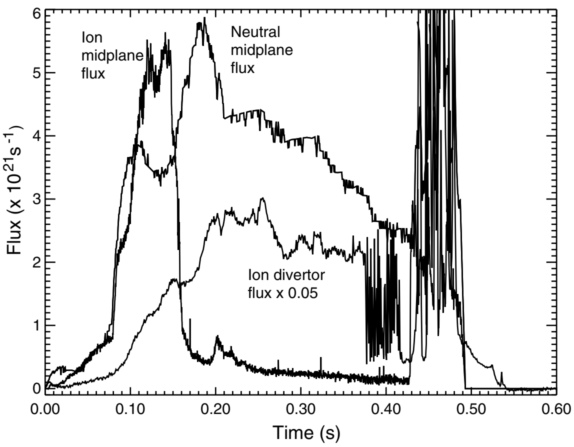

Fig. 5. Estimated ion and neutral fluxes for the discharge shown in Fig. 2.

5. Summary

Particle balance and core fueling efficiencies of low and high field side gas fueling of L-mode ohmic and NBI heated plasmas have been compared using an analytical zero-dimensional particle balance model and measured ion and neutral fluxes. Gas fueling efficiencies are in the range of 0.05–0.20 and do not depend on discharge magnetic configuration or poloidal location of the injector. Higher densities are achieved using LFS + HFS fueling with lower average injection rates. The particle balance model indicates that the addition of a pseudo-constant HFS fueling source results in a reversal of the wall loading rate. Initial particle source estimates obtained from neutral pressure and spectroscopic measurements indicate that in diverted discharges ion flux in the divertor greatly exceeds ion and neutral fluxes in the main chamber. Present analysis provides the basis for detailed fluid modeling of edge particle flows and the analysis of particle confinement properties of L- and H-mode plasmas.

Acknowledgements

The authors would like to thank G. Zimmer for the software development. W. Blanchard, R. Gernhardt, and P. Sichta are acknowledged for the engineering support. This research was supported by the US Department of Energy under contracts no. DE-AC02-76CH03073, DE-AC05-00OR22725, and W-7405-ENG-36.

References

[1] R. Akers, A. Bond, R. Buttery, P. Carolan, G.F. Counsell, G. Cunningham, S. Fielding, C. Gimblett, M. Gryaznevich, J. Hastie, P. Helander, T. Hender, P. Knight, C. Lashmore-Davies, G.P.M. Ison, T. Martin, K. McClements, A.M. Ris, M. O'Brien, C.R. Ro, C. Roach, D. Robinson, A. Sykes, G. Voss, M. Walsh, H. Wilson, F. Zaitsev, Nucl. Fusion 40 (6) (2000) 1223.

[2] G. Federici, C.H. Skinner, J.N. Brooks, J.P. Coad, C. Grisola, A.A. Haasz, A. Hassanein, V. Philipps, C.S. Pitcher, J. Roth, W.R. Wampler, D.G. Whyte, Nucl. Fusion 41 (12R) (2001) 1267.

[3] A.R. Field, E.R. Arends, P.G. Carolan, P.J. Catto, N.J. Conway, G. Cunningham, T. Fullop, P. Helander, B. Lloyd, H. Meyer, M.J. Walsh, the MAST and NBI teams, in: Proceedings of the 29th EPS Conference on Plasma Physics and Controlled Fusion, Montreux, Switzerland, 2002.

[4] R. Maingi, G.L. Jackson, M.R. Wade, M.A. Mahdavi, P.K. Mioduszewski, G. Haas, M.J. Schaffer, J.T. Hogan, C.C. Klepper, Nucl. Fusion 36 (2) (1996) 245.

[5] C.H. Skinner, H.W. Kugel, R. Maingi, W.R. Wampler, W. Blanchard, M.G. Bell, R.E. Bell, D.A. Gates, S.M. Kaye, P. LaMarche, B.P. LeBlanc, J.E. Menard, D. Muller, H.K. Na, N. Nishino, F. Paoletti, S.F. Paul, S.A. Sabbagh, V.A. Soukhanovskii, D. Stutman, Nucl. Fusion 42 (2002) 329.

[6] H.W. Kugel, V.A. Soukhanovskii, M. Bell, W. Blanchard, D. Gates, B. LeBlanc, R. Maingi, D. Muller, H.K. Na, S. Paul, C.H. Skinner, D. Stutman, W.R. Wampler, in: Proceedings of the 15th International Conference on Plasma Surface Interactions in Controlled Fusion Devices, Gifu, Japan, 27–31 May 2002.

[7] M.V. Umansky, S.I. Krasheninnikov, B. LaBombard, J.L. Terry, Phys. Plasmas 5 (1998) 3373.

[8] B. LaBombard, M.V. Umansky, R.L. Boivin, J.A. Goetz, J. Hughes, B. Lipschultz, D. Mossessian, C.S. Pitcher, J.L. Terry, Nucl. Fusion 40 (12) (2000) 2041.

[9] A.Y. Pigarov, S.I. Krasheninnikov, T.D. Rignlien, M.J. Schaffer, W.P. West, Phys. Plasmas 9 (2002) 1287.